

MYELOID NEOPLASIA

The Src and c-Kit kinase inhibitor dasatinib enhances p53-mediated targeting of human acute myeloid leukemia stem cells by chemotherapeutic agents

Cedric Dos Santos,¹ Tinisha McDonald,¹ Yin Wei Ho,¹ Hongjun Liu,¹ Allen Lin,¹ Stephen J. Forman,² Ya-Huei Kuo,¹ and Ravi Bhatia¹

¹Division of Hematopoietic Stem Cell and Leukemia Research and ²Department of Hematology and Hematopoietic Cell Transplantation, City of Hope National Medical Center, Duarte, CA

Key Points

- SRC family kinases are activated in AML stem/progenitor cells and contribute to AML stem cell survival and proliferation.
- Combined inhibition of SFKs and c-KIT with dasatinib enhances p53-mediated elimination of AML stem cells.

The SRC family kinases (SFKs) and the receptor tyrosine kinase c-Kit are activated in human acute myeloid leukemia (AML) cells. We show here that the SFKs LYN, HCK, or FGR are overexpressed and activated in AML progenitor cells. Treatment with the SFK and c-KIT inhibitor dasatinib selectively inhibits human AML stem/progenitor cell growth in vitro. Importantly, dasatinib markedly increases the elimination of AML stem cells capable of engrafting immunodeficient mice by chemotherapeutic agents. In vivo dasatinib treatment enhances chemotherapy-induced targeting of primary murine AML stem cells capable of regenerating leukemia in secondary recipients. Our studies suggest that enhanced targeting of AML cells by the combination of dasatinib with daunorubicin may be related to inhibition of AKT-mediated human mouse double minute 2 homolog phosphorylation, resulting in enhanced p53 activity in AML cells. Combined treatment using dasatinib and chemotherapy provides a novel approach to increasing p53 activity and enhancing targeting of AML stem cells. (*Blood*. 2013;122(11):1900-1913)

Introduction

Acute myeloid leukemia (AML) is a clonal hematopoietic disorder characterized by an accumulation of immature myeloid cells. Current treatment of AML remains unsatisfactory, with a 5-year relapse-free survival rate lower than 50% in younger adults and 12% in elderly adults.¹ Leukemic hematopoiesis, similar to normal hematopoiesis, is hierarchically organized and is propagated by small populations of leukemia stem cells (LSC). The inability to eliminate LSC, which are relatively insensitive to common AML therapies, likely contributes to relapse after treatment.¹ LSC share several features with normal hematopoietic stem cells (HSC), including quiescence, self-renewal capability, and Lin⁻CD34⁺CD38⁻ phenotype.^{2,3} However, LSC are also detected in AML cells coexpressing CD38 and/or lacking CD34 expression.^{4,5}

Development of strategies to enhance AML LSC targeting is impeded by limited understanding of mechanisms underlying LSC maintenance. AML arises through at least 2 types of cooperative mutations,⁶ which confer growth and proliferative advantages and impair hematopoietic differentiation. Mutations in receptor tyrosine kinases (RTKs), such as Fms-like tyrosine kinase 3 (FLT3) or c-KIT, are frequently seen in AML.⁷ Activating *c-KIT* mutations are associated with AML with core-binding factor (CBF) abnormalities. In addition, wild-type c-KIT is often overexpressed and phosphorylated in human AML cells, and the c-KIT ligand stem cell factor stimulates proliferation of AML cells.⁸ In addition to RTKs, cytoplasmic

tyrosine kinases such as the SRC family tyrosine kinases (SFKs) regulate multiple processes important for tumor progression, including cell adhesion, migration, proliferation, and survival.^{9,10} The 9 SFK members, c-SRC, YES, FYN, LYN, LCK, HCK, FGR, BLK, and YRK, locate to the plasma membrane, particularly lipid rafts, via posttranslational modifications.⁹ SFK contribute to cell survival and drug resistance in other hematological malignancies.^{11,12} We have shown that LYN, HCK, and FGR are abnormally activated and contribute to AML cell growth and survival.¹³ Recently, HCK was reported to be activated in AML LSC.¹⁴ Other groups have shown that LYN is activated downstream of the *FLT3-internal tandem duplication (ITD)* mutation¹⁵ and that SFKs promote survival of AML cell lines.¹⁶ Nonetheless, the role of SFKs in AML LSC maintenance and resistance to conventional treatment has not been studied.

Here we investigated the activity of SFKs and c-KIT in AML stem and progenitor cells. We used RNAi and the small-molecule inhibitor dasatinib to target SFK and c-KIT in AML and normal stem/progenitor cells. Dasatinib is approved for treatment of chronic myeloid leukemia and efficiently inhibits Breakpoint Cluster Region-Abelson, SFKs, c-KIT, and platelet-derived growth factor receptor-beta at nanomolar concentrations.¹⁷ We evaluated whether combination of dasatinib with the chemotherapeutic agents daunorubicin (DNR) and cytarabine (Ara-C) could enhance elimination of AML stem/progenitor cells, and we studied the underlying mechanisms.

Submitted November 9, 2012; accepted July 18, 2013. Prepublished online as *Blood* First Edition paper, July 29, 2013; DOI 10.1182/blood-2012-11-466425.

Y.-H.K. and R.B. contributed equally to this study.

The online version of this article contains a data supplement.

The publication costs of this article were defrayed in part by page charge payment. Therefore, and solely to indicate this fact, this article is hereby marked "advertisement" in accordance with 18 USC section 1734.

© 2013 by The American Society of Hematology

Materials and methods

Patients samples and reagents

Peripheral blood (PB) or bone marrow (BM) samples from newly diagnosed, relapsed, or treatment refractory patients with AML (Table 1); cord blood (CB) samples from healthy donors; and PB stem cells (PBSC) from allogeneic transplant donors were obtained under a City of Hope Cancer Center Institutional Review Board–approved protocol, in accordance with the Declaration of Helsinki. All donors signed informed consent forms. Mononuclear cells (MNCs) were isolated using Ficoll-Hypaque separation.¹⁸ CD34⁺ or Lin-depleted cells were selected using immunomagnetic columns (Miltenyi Biotech). A 10-mM stock solution of dasatinib (Bristol-Myers Squibb) in dimethylsulfoxide was stored at –20°C. Ara-C and DNR were purchased from the City of Hope pharmacy, and LY294002 from Calbiochem.

Cell culture

Cells were cultured in serum-free medium (StemCell Technologies) supplemented with low growth factors at concentrations similar to those found in long-term bone marrow culture conditioned medium (200 pg/mL granulocyte-macrophage colony-stimulating factor, 1 ng/mL granulocyte colony-stimulating factor, 200 pg/mL stem cell factor, 50 pg/mL leukemia inhibitory factor, 200 pg/mL macrophage-inflammatory protein-1 α , and 1 ng/mL interleukin 6).¹⁸

Intracellular staining for phosphorylated SFK (Y416)

Leukemic cells were stained with an Ag-presenting cell (APC)-Cyano dye 7–labeled lineage cocktail (including anti-CD2, anti-CD3, anti-CD7, anti-CD10, and anti-CD19 antibodies), anti-CD34-PE-Cyano dye 7, and anti-CD38-APC antibodies (eBioscience); fixed and permeabilized (Cytofix/Cytoperm; Beckman Coulter); labeled with Alexa Fluor 488 conjugated antiphospho SFK (Y416) (Cell Signaling Technology); and analyzed by flow cytometry (LSRII; BD Biosciences). Fluorescence minus one controls were used to set gates. Results were expressed as ratio of mean fluorescence intensity for antiphospho SFK to mouse immunoglobulin G1 kappa control.

Progenitor assays

Colony-forming cells (CFC). CD34⁺ cells cultured with or without drug were plated in methylcellulose progenitor culture, and hematopoietic colonies were counted after 14 days.¹⁸

Long-term culture-initiating cell (LTC-IC). Cells were plated with or without dasatinib in long-term BM culture medium on M2-10B4 murine fibroblast feeders subcultured in 96-well plates. Cultures were maintained at 37°C with 5% CO₂ and fed weekly. After 6 weeks, wells were overlaid with CFC culture medium and scored as positive or negative for CFC after 2 weeks. LTC-IC frequency was calculated using L-Calc software (StemCell Technologies).¹⁸

Cell cycle analysis

CD34⁺ cells were cultured for 48 hours in high growth factors (HGF) (Iscove modified Dulbecco medium with 30% fetal bovine serum and 3 U/mL erythropoietin, 5 ng/mL stem cell factor, 20 ng/mL granulocyte-macrophage colony-stimulating factor, 20 ng/mL granulocyte colony-stimulating factor, and 5 ng/mL interleukin 3), fixed with 4% paraformaldehyde, permeabilized with 70% methanol, and stained with Ki67-fluorescein isothiocyanate (BD Pharmingen) and 7-aminoactinomycin D (7-AAD; BD Pharmingen).¹⁹ After excluding sub-G₀ cells, Ki67⁺-AAD[–] (G₀), Ki67⁺-AAD[–] (G₁), and Ki67⁺-AAD⁺ cells (S/G₂/M phase) were enumerated.

Carboxyfluorescein diacetate, succinimidyl ester labeling

CD34⁺ cells were labeled with carboxyfluorescein diacetate, succinimidyl ester (CFSE; Molecular Probes), incubated overnight in HGF to release unbound dye, and cultured in HGF for 72 hours. Cell division was analyzed by flow cytometry.²⁰ The parent generation was set on the basis of a cell aliquot fixed with paraformaldehyde after CFSE labeling. A proliferation index (PI)

was calculated using ModFit LT 3.0 software (Verity), simplifying comparison between samples and conditions.

Apoptosis analysis

Cells were labeled with CD34, CD45 Annexin V-APC (BD Pharmingen), and 4,6 diamidino-2-phenylindole and analyzed by flow cytometry (LSRII; BD Biosciences). Apoptotic cells were defined as Annexin V-APC⁺.

Real-time quantitative polymerase chain reaction analysis

Total RNA was extracted using the RNeasy micro kit (Qiagen) and cDNA generated using the Superscript III First-Strand Synthesis System (Invitrogen). Quantitative RT-PCR was performed using a 7900 HT ABI PRISM Real-Time PCR System and TaqMan gene expression assays (Applied Biosystems). Results were normalized to endogenous control β 2-microglobulin (*b2m*) expression.

RNA interference

CD34⁺ cells were transfected using the Amaxa 96-well shuttle (Amaxa). 5 × 10⁴ cells were suspended in Nucleofector solution and transfected with siRNA in triplicate, using the human CD34⁺ cell 96-well Nucleofector kit, program E0-100. For p53 siRNA experiments, AML samples transfected with control and p53 siRNA were cultured with or without dasatinib (200 nM) plus DNR (50 nM) for 2 days, and apoptosis was assessed.

Western blot analysis

Proteins were resolved using 4% to 12% v-polyacrylamide gel electrophoresis Bis-Tris gels (Invitrogen) and transferred to nitrocellulose membranes (Millipore). After blocking in PBS-0.1% Tween 20% to 5% bovine serum albumin, membranes were immunostained with appropriate antibodies and horseradish peroxidase-conjugated secondary antibodies (Jackson Immuno-Research Laboratories) and visualized with an enhanced chemiluminescence detection system (Superfemto kit; Pierce Biotechnology).

Engraftment of human cells in immunodeficient mice

MNCs were T-cell-depleted, using immunomagnetic columns (Miltenyi Biotech); cultured for 48 hours with or without drug; and transplanted via the tail vein into 6- to 8-week-old nonobese diabetic-severe combined immunodeficiency (*SCID*) interleukin 2 γ ^{null} (NSG) mice irradiated at 300 cGy (The Jackson Laboratories). Mice were analyzed 12 weeks posttransplant for human CD45⁺ cell engraftment, using flow cytometry.^{2,4,21} Specific human subsets were analyzed, using antibodies to human CD34, CD33, CD15, CD14, CD11b, CD3, and CD19 (BD Biosciences). Mouse care and experimental procedures were in accordance with protocols approved by the Institutional Animal Care and Use Committee.

In vivo treatment in the murine leukemia model

To obtain leukemic cells, *C57Bl6 Cbfb^{56M/+} Mx1-Cre* mice treated with polyinosinic-polycytidylic acid (Sigma-Aldrich)²² were treated with fluorouracil (150 mg/kg). BM progenitors were isolated after 5 days, transduced with murine stem cell virus-internal ribosome entry site-green fluorescent protein-myeloproliferative leukemia virus oncogene retrovirus, and transplanted into wild-type recipients.²³ After leukemia development, BM cells were cryopreserved. For therapeutic studies, leukemic cells were injected into sublethally irradiated (650 cGy) 6- to 8-week-old C57BL/6N mice (National Cancer Institute, Frederick National Laboratory). Mice were treated with dasatinib, Ara-C, and doxorubicin, or dasatinib combined with Ara-C and doxorubicin, as indicated. Leukemic engraftment was analyzed by enumerating green fluorescent protein (GFP)⁺ cells.²² Secondary transplantation was performed by transferring BM cells from treated mice into sublethally irradiated recipients.

Statistical analysis

Data from independent experiments were reported as mean \pm SEM. Statistical significance of differences between treatment groups was

Table 1. Clinical characteristics of AML patients

Sample	Age, years	Sex	FAB	WBC	BM/PB	Disease status	Risk category	Cytogenetics	Fit3 mutn	%Blasts (PB)	%Blasts (BM)
AML 1	61	F	M1	82.9	BM	Untreated	I	t(1;7)	NA	87	90
AML 2	47	F	M4	50.8	PB	Untreated	B	inv(16)	Neg	67	90
AML 3	61	M	NA	1.8	PB	Untreated	I	+13, +21	NA	26	
AML 4	56	F	M2	38.8	PB	Untreated	B	inv(16), +8	NA	63	44
AML 5	69	M	NA	18.2	PB	Untreated	P	del(5q), inv(1q), -17	NA	4	18
AML 6	54	M	M4	14.2	PB	Untreated	P	Complex	Neg	3	60
AML 7	54	M	M4	14.2	BM	Untreated	P	Complex	Neg	3	60
AML 8	40	F	NA	8.6	PB	Relapsed	B	t(8;21); -	NA	80	
AML 9	39	F	M2	6.5	BM	Untreated	B	t(8;21),	NA	32	40
AML 10	51	M	NA	13.4	BM	Untreated	B	Inv(16), +8, +21	NA	70	75
AML 11	57	M	M4	82.8	PB	Relapsed	B	t(16;16), +21, t+22	NA	94	67
AML 12	70	M	NA	114.7	PB	Relapsed	I	t(1;7), t(14;15)	NA	90	
AML 13	71	M	NA	32.4	PB	Relapsed	I	del(20)	NA	90	64
AML 14	62	F	M6	2.7	BM	Persistent	P	Complex	NA	20	60
AML 15	66	F	NA	8.9	BM	Relapsed	P	Complex	NA	1	90
AML 16	63	F	M6	1.5	BM	Persistent	P	Complex	NA	4	33
AML 17	58	M	M4	27.3	PB	Relapsed	I	Normal	NA	89	
AML 18	81	F	NA	20.5	BM	Refractory	P	Complex	NA	62	72
AML 19	23	M	M3	80.7	PB	Untreated	I	t(7;11)	Neg	28	
AML 20	41	M	M4	11.9	BM	Relapsed	P	Complex	NA	5	62
AML 21	83	F	NA	31.1	BM	Persistent	I	Normal	NA	33	33
AML 22	76	M	NA	6.9	BM	Untreated	I	Normal	NA	25	64
AML 23	42	M	NA	5.4	PB	Persistent	I	inv(13), del(3)	NA	80	
AML 24	32	M	M5	22.2	PB	Induction failure	P	t(9;11), del(9p)	Neg	61	
AML 25	64	F	M0	6.2	PB	Persistent	I	t(2;8), t(3;12;7), 3q26.2	NA	96	
AML 26	41	M	M4	30.5	BM	Relapsed	P	Complex	NA	17	53
AML 27	74	F	NA	63.3	PB	Untreated	B	Normal	Neg	76	
AML 28	74	F	M4	10.5	PB	Persistent	P	Complex	NA	74	
AML 29	46	F	NA	3.2	PB	Relapsed	I	Trisomy 8	NA	3	30
AML 30	81	F	NA	30.42	PB	Persistent	P	Complex	NA	33	
AML 31	44	F	NA	12.1	PB	Relapsed	I	del(17p), dic(11;7),	NA	47	0
AML 32	74	F	NA	1.9	BM	Persistent	I	Trisomy 8, Tetrasomy 8	NA	1	21.5
AML 33	31	F	NA	63.6	PB	Relapsed	P	del(11q),t(3;18)	Pos	81	
AML 34	56	F	NA	7.7	BM	Untreated	I	Normal	NA	28	32.5
AML 35	69	M	M4	22	PB	Untreated	P	+8, del(13q)	Pos	75	
AML 36	46	F	M1	30	PB	Relapsed	P	del(10), t(10;11)	Pos	82	
AML 37	58	M	NA	12.1	PB	Induction failure	I	t(3;6),del(7)	Pos	60	
AML 38	42	F	M3	9.1	PB	Untreated	B	t(15;17)	Neg	64	95
AML 39	28	M	NA	49.76	PB	Relapsed	I	Normal	NA	61	
AML 40	58	F	M1	21.8	PB	Untreated	I	Normal	NA	56	74
AML 41	37	M	M4/M5	30.5	PB	Induction failure	P	Normal	Pos	24	
AML 42	58	F	NA	15.4	PB	Relapsed	P	inv(3q), add(16)	NA	58	
AML 43	61	F	M2	8.4	PB	Persistence	P	Complex	NA	63	
AML 44	59	F	M5	22.7	PB	Untreated	B	Normal	Neg	7	50
AML 45	55	F	NA	11	PB	Relapsed	P	Inv(3), add (16)	Neg	57	
AML 46	55	M	M1/M2	136.4	PB	Persistent	B	Normal	Neg	94	
AML 47	24	M	NA	4.3	BM	Persistent	I	Two clonal abnormalities t(7;11)	NA	0	1
AML 48	56	M	M1/M2	43.2	PB	Untreated	I	Trisomy 4	NA		90
AML 49	21	F	NA	71.1	PB	Relapsed	P	Complex	Neg	93	
AML 50	83	M		6.5	PB	Untreated	P	Complex abnormalities,	NA	53	
AML 51	23	M	M1	1.5	PB	Refractory	P	Complex	NA	14	
AML 52	74	F	NA	4.5	PB	Refractory	P	Normal cytogenetics,	NA	96	
AML 53	64	M	NA	15.4	BM	Untreated	P	t(9;22)	NA	15	22.5
AML 54	61	M	NA	7.6	PB	Induction failure	P	Complex abnormalities, including del(5q), del(6q), del(17p)	NA	72	80
AML 55	57	M	M-4	82.8	BM	Relapsed	B	t(16;16), trisomy 21, trisomy 22	NA	94	70
AML 56	73	M	M-0	42.5	BM	Untreated	P	del(5q), trisomy 8, trisomy 13, del(17p)	Neg	87	95
AML 57	38	M	NA	1.8	BM	Relapsed	I	Normal Cytogenetic	NA	0	20
AML 58	30	F	NA	12.7	PB	Untreated	I	Normal Cytogenetic	NA	75	ND
AML 59	68	M	NA	8.4	BM	Relapsed	I	Trisomy 13, Trisomy 21	Neg	10	58
AML 60	67	M	NA	16.5	BM	Persistent	I	Trisomy 8, Tetrasomy 8	NA	75	84
AML 61	73	F	NA	22.7	BM	Untreated	I	Trisomy 8, Tetrasomy 8	NA	2	23

B, better risk; F, female; FAB, French-American-British classification; FLT3 mutn, FLT3-ITD internal tandem duplication mutation; I, Intermediate risk; M, male; NA, nonavailable; Neg, negative; P, poor risk; Pos, positive; WBC, white blood cell count (cells per microliter).

Table 1. (continued)

Sample	Age, years	Sex	FAB	WBC	BM/PB	Disease status	Risk category	Cytogenetics	Flt3 mutn	%Blasts (PB)	%Blasts (BM)
AML 62	23	F	NA	64.8	PB	Relapsed	P	Complex abnormalities, including del(11p)	Pos	84	ND
AML 63	47	M	M-4	31.3	PB	Relapsed	P	Complex abnormalities in 3 cell lines	NA	91	ND
AML 64	79	F	NA	1.9	PB	Refractory	P	monosomy 7, trisomy 21	NA	0	ND
AML 65	74	F	M4	5.3	BM	Relapsed	P	Complex abnormalities, including monosomy 7, del (7q), RUNX1, MLL loss,	NA	37	86
AML 66	61	F	NA	44.7	PB	Untreated	P	Complex abnormalities,	NA	51	80
AML 67	47	M	M-0	5.9	PB	Relapsed	P	Complex abnormalities, including monosomy 8, loss of ABL1/ASS	NA	54	ND
AML 68	28	M	NA	49.7	PB	Relapsed	I	Normal Cytogenetic	NA	61	ND
AML 69	57	M	NA	73.3	Leukocytes	Relapsed	P	Massive hyperdiploidy (> 50 chromosomes)	Neg	93	ND
AML 70	74	F	NA	23.6	BM	Persistent	I	Trisomy 8, Tetrasomy 8	NA	12	47
AML 71	38	M	M4/M5	1.3	PB	Induction failure/refractory	P	Trisomy 8, del(9q), t(2;18), trisomy 13	Pos	41	8
AML 72	48	F	NA	14.9	PB	Persistence	P	del(6), t(10;11)	Pos	61	60

B, better risk; F, female; FAB, French-American-British classification; FLT3 mutn, FLT3-ITD internal tandem duplication mutation; I, Intermediate risk; M, male; NA, nonavailable; Neg, negative; P, poor risk; Pos, positive; WBC, white blood cell count (cells per microliter).

determined using a 2-tailed Student *t* test. Drug combination experiments were analyzed using analysis of variance (ANOVA), followed by a posttest.

Results

Increased SFK phosphorylation in AML stem and progenitor cells

We assessed SFK activity in Lin⁻CD34⁺CD38^{dim/-}, Lin⁻CD34⁺CD38⁺, and Lin⁻CD34⁻ cells from patients with AML (*n* = 56) and healthy donors (*n* = 12, 3 BM, 4 CB, 5 PBSC) by flow cytometry after labeling with an antibody recognizing the Y416 autophosphorylation site on active forms of SFKs.^{10,13} There were no significant differences in *p*-SFK between adult BM, PBSC, and CB. Each AML subpopulation displayed significantly higher *p*-SFK compared with normal cells (Figure 1A; supplemental Figure 1A-B, available on the *Blood* Web site). Results of flow cytometry correlated well with Western blot (supplemental Figure 1C). *p*-SFK expression was similar in samples from patients with good-, intermediate-, and bad-risk cytogenetics, per National Comprehensive Cancer Center Network guidelines (Figure 1B),²⁴ and in patients with or without the *FLT3-ITD* mutation (not shown). Most AML samples displayed low levels of phosphorylation of the negative regulatory Y527 site compared with the activation-associated Y416 site,^{9,10} which is consistent with increased SFK activation.¹³ We found consistent LYN and HCK expression and variable FGR expression in AML CD34⁺ cells, indicating that AML samples coexpress multiple SFK, with most expressing both HCK and LYN and with a subset also expressing FGR.

Knockdown of LYN, HCK, and FGR or c-KIT impairs AML progenitor survival and proliferation

We used siRNA-mediated knockdown to evaluate the relative role of LYN, HCK, and FGR in AML CD34⁺ cell survival and proliferation. We confirmed more than 70% transfection efficiency, using fluorescent-labeled siRNA (supplemental Figure 2A). LYN, HCK, and FGR siRNA significantly inhibited target mRNA expression (Figure 2A), SFK phosphorylation (Figure 2A), survival (Figure 2B;

supplemental Figure 2B), and CFC growth (Figure 2C) compared with control siRNA. Effects were more marked for LYN and HCK compared with FGR siRNA. Combined treatment with siRNA to LYN HCK and FGR (LHF) resulted in increased apoptosis (Figure 2D) and CFC inhibition (Figure 2E). We also show that siRNA to c-KIT significantly inhibited c-KIT mRNA expression (Figure 2A), survival (Figure 2D), and CFC growth (Figure 2E) compared with control siRNA. A second set of siRNAs targeting different LYN, HCK, FGR, and c-KIT sequences resulted in a similar increase in apoptosis (supplemental Figure 2C), decrease in CFC (supplemental Figure 2D), and target gene knockdown (*n* = 5; supplemental Figure 2E). The siRNAs used primarily inhibited expression of the targeted SFK (supplemental Figure 2F).

The SFK and c-KIT inhibitor dasatinib selectively inhibits AML primitive and committed progenitors

Because SFKs have redundant signaling functions,⁹ targeting multiple SFKs with a small-molecule inhibitor such as dasatinib may be more effective in inhibiting AML stem/progenitor growth than targeting individual SFKs. Dasatinib also inhibits c-KIT activation,²⁵ which could be an added advantage. Exposure to dasatinib (*n* = 6; Figure 2F) inhibited SFK phosphorylation in AML CD34⁺CD38⁻ and AML CD34⁺CD38⁺ (representative data; supplemental Figure 2G). Dasatinib inhibited SFK and c-KIT phosphorylation (detected using a phospho-c-Kit [Y719] antibody) on Western blotting after 2 hours (Figure 2G) and 48 hours (Figure 2H). Similarly, analysis of dose and concentration response by flow cytometry (supplemental Figure 3A) showed significant *p*-SFK inhibition with dasatinib 100 nM at 2 hours and at 200 nM at 48 hours. Although dasatinib concentrations required for SFK inhibition in AML CD34⁺ cells are higher than those required to inhibit purified SFK proteins, they are within the range of plasma levels achieved in patients.²⁶

Dasatinib resulted in dose-dependent inhibition of AML compared with normal CFC growth (Figure 3A). We observed maximal CFC growth inhibition with 200 nM dasatinib. Dasatinib also reduced AML primitive progenitor growth in LTC-IC assays (Figure 3B) without affecting normal progenitor growth (Figure 3B). Dasatinib significantly increased apoptosis of AML compared with normal CD34⁺ cells (Figure 3C; supplemental Figure 3B). Cells

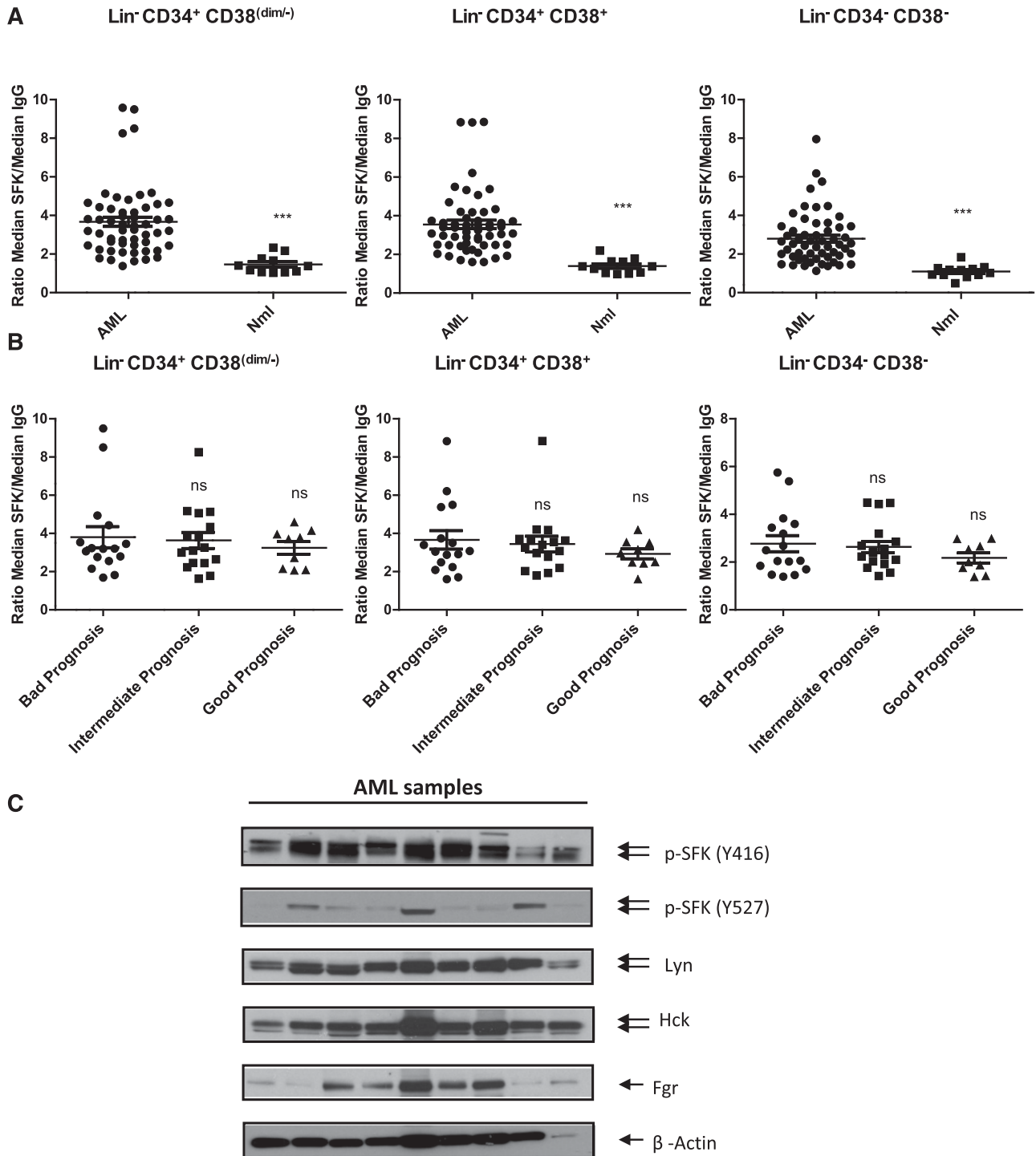


Figure 1. SFKs are constitutively activated in AML stem and progenitor cells independent of the cytogenetic risk. (A) Flow cytometry analysis of SFKs using a phosphospecific antibody recognizing the activated form of SFK members (Y416) in normal (Nml) or AML stem/primitive cells Lin⁻ CD34⁺ CD38^(dim/-), AML progenitors cells Lin⁻ CD34⁺ CD38⁺, and AML more mature cells Lin⁻ CD34⁻ CD38⁻. Scatter plots comparing SFK phosphorylation (expressed as ratio of median fluorescence intensity for pSFK vs isotype control) in Lin⁻ CD34⁺ CD38^(dim/-), Lin⁻ CD34⁺ CD38⁺, and Lin⁻ CD34⁻ CD38⁻ cells from AML (n = 56) and normal samples (n = 12; 3 BM, 4 CB, and 5 PBSC samples; ***P < .002). (B) Scatter plots comparing SFK phosphorylation in primary AML patients according to their prognostic risk category (bad, intermediate, and good prognosis). ns, non significant. (C) Western blots analysis for fresh or thawed CD34⁺ AML samples. Indicated antibodies are listed, and β-actin was used as a loading control. Results shown are representative of 9 AML samples analyzed.

remaining after 48 hours of treatment showed persistent inhibition of SFK and downstream pathways (Figure 2H; supplemental Figure 3C). SFK or c-KIT activity was not affected by low vs high GF culture conditions (supplemental Figure 3D). Dasatinib significantly

inhibited AML CD34⁺ cell division assessed by CFSE labeling (Figure 3D; supplemental Figure 3E) and significantly increased cells in G₀ and reduced cells in S/G₂/M phase on Ki67/7AAD labeling (Figure 3E; supplemental Figure 3F).

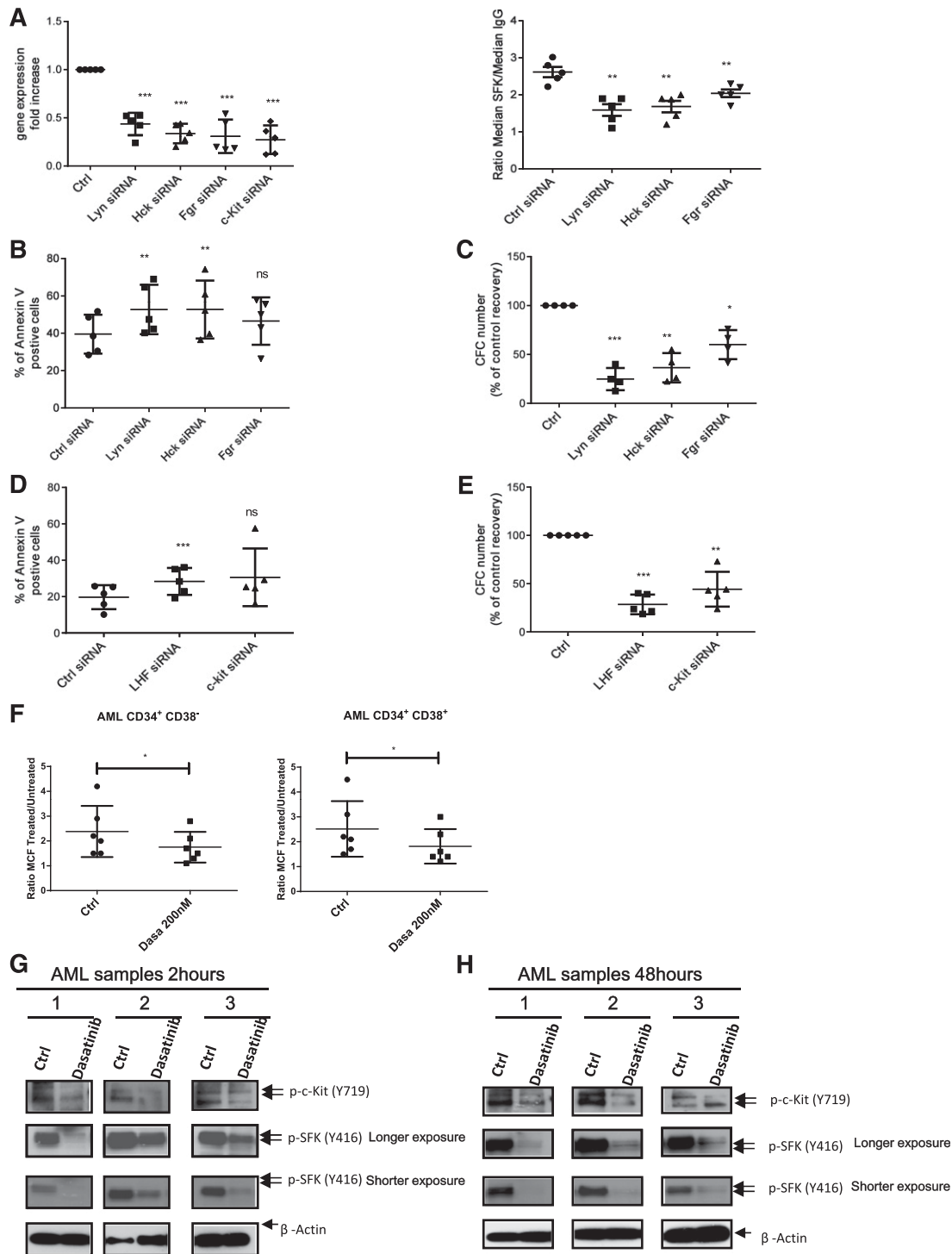


Figure 2. SFK and c-KIT knockdown using siRNA inhibits survival and growth of primitive and committed AML progenitors. (A) LYN, HCK, FGR, and c-KIT gene expression fold change in AML CD34⁺ cells (n = 5; ***P < .001) (left). (right) Detection of SFKs phosphorylation by flow cytometry 72 hours postnucleofection (n = 5; **P < .01). Results shown represent the mean ± SEM of 5 AML samples. (B) AML CD34⁺ apoptosis (n = 5) 72 hours postnucleofection. Results are presented as mean ± SEM of Annexin V-positive cells for 5 AML samples. ns, non significant; **P < .01. (C) CFC assay 72 hours postnucleofection (n = 4). Results are presented as percentage of control and are mean ± SEM for 4 AML samples. *P < .05; **P < .01; ***P < .001. (D) AML CD34⁺ apoptosis (n = 5; ***P < .001) 72 hours postnucleofection with indicated siRNA. Results represent mean ± SEM of Annexin V-positive cells. ns, non significant; ***P < .001. (E) CFC assay 72 hours postnucleofection (n = 5). Results shown are percentage of control and represent mean ± SEM. **P < .01; ***P < .001. (F) SFK phosphorylation 2 hours after dasatinib treatment (200 nM) for AML CD34⁺CD38⁻ (left; *P < .05) and AML CD34⁺CD38⁺ cells (right; *P < .05). Results are representative of 6 AML samples. (G-H) Western blot analysis of c-KIT and SFK phosphorylation in CD34⁺ cells from 3 AML patients cultured for 2 hours (G) or 48 hours (H) without or with 200 nM dasatinib. Results shown are representative of 6 AML samples.

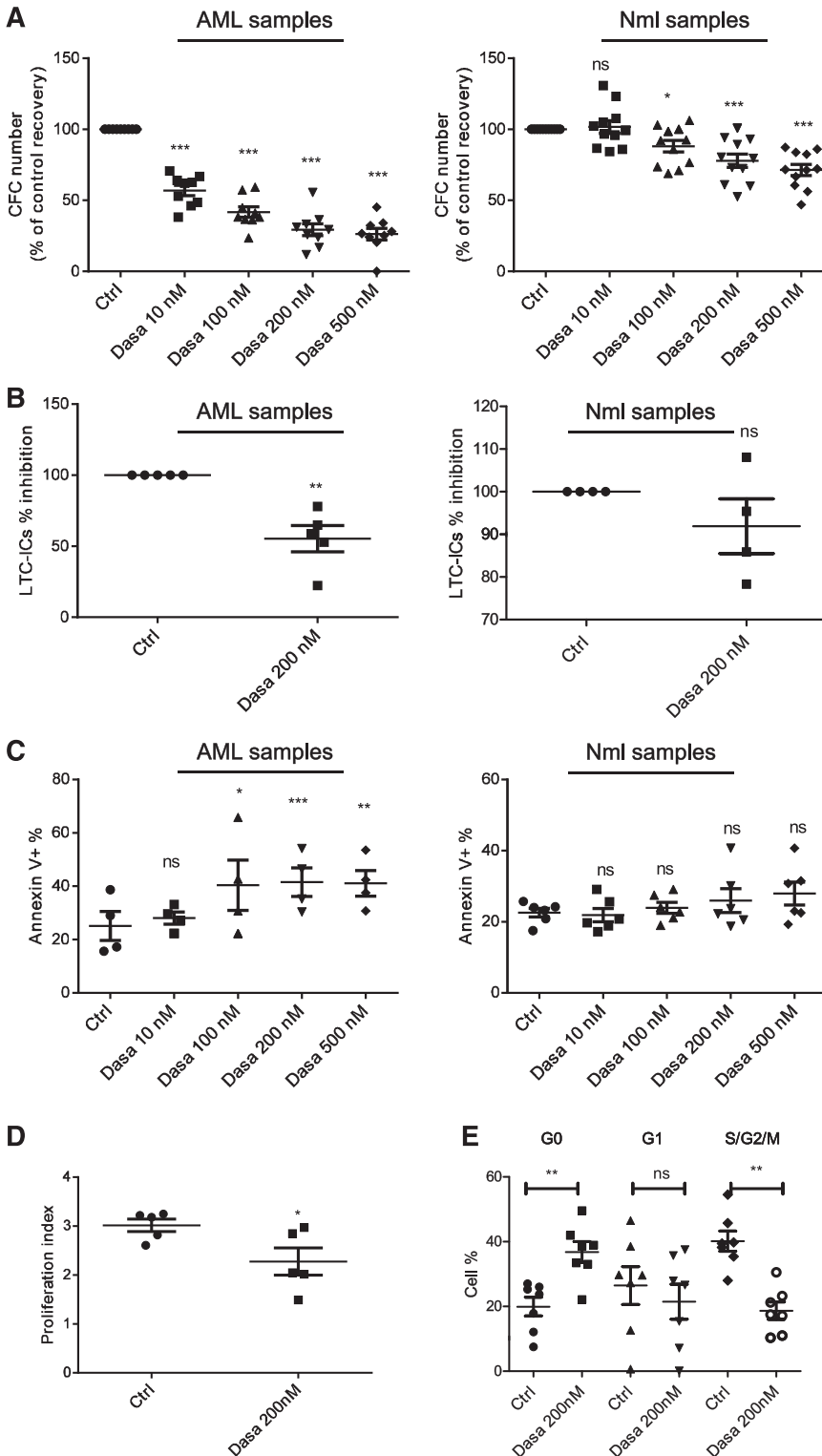


Figure 3. Effect of SFK inhibition using dasatinib on apoptosis and growth of primitive and committed progenitors. (A) CFC assay of AML (n = 9; left; ****P* < .001) or normal CD34⁺ cells (n = 11; 6 PBSC and 5 CB; ns, nonsignificant; **P* < .05; ****P* < .001) exposed to increasing doses of dasatinib for 48 hours. Results shown are presented as percentage of control (mean ± SEM). (B) LTC-IC assays of AML (left; n = 5; ***P* < .01) or normal CD34⁺ (right; n = 4; 2 PBSC and 2 PBSC; ns, nonsignificant) cells treated with dasatinib. The percentage inhibition of LTC-IC frequency relative to untreated controls is shown for AML. (C) Apoptosis of AML (n = 4) and normal CD34⁺ (n = 6; 3 PBSC, 3 CB) cells cultured for 48 hours with indicated concentrations of dasatinib. Results shown are presented as mean ± SEM of Annexin V-positive cells in treated vs untreated cells. ns, non significant; **P* < .05; ***P* < .01; ****P* < .001. (D) PI of AML CD34⁺ cells determined by CFSE labeling assays. The PI was determined using ModFit software and proliferation indices were normalized to untreated controls. Compiled data for proliferation of 5 AML is shown (**P* < .05). (E) Cell cycle analysis of AML progenitors CD34⁺ (n = 7), using Ki-67 and 7-AAD staining (ns, nonsignificant; ***P* < .01).

Dasatinib enhances inhibition of AML progenitors by chemotherapeutic agents

We evaluated whether dasatinib treatment enhanced AML stem/progenitor cell targeting by DNR and Ara-C. A combination of dasatinib (200 nM) with DNR (50 nM) or Ara-C (50 nM) for 72 hours resulted in significantly greater inhibition of AML CD34⁺ cell proliferation (Figure 4A-B) and apoptosis (Figure 4C) compared with dasatinib, DNR, or Ara-C alone. Combination of dasatinib

with DNR or Ara-C also enhanced CFC inhibition compared with dasatinib, DNR, and Ara-C alone (Figure 4D).

Combination of dasatinib with chemotherapy enhances targeting of AML NSG mouse repopulating cells

We assessed whether dasatinib could enhance targeting of AML LSC capable of engrafting NSG mice by chemotherapeutic agents. T-cell-depleted MNCs cultured with dasatinib (200 nM), DNR

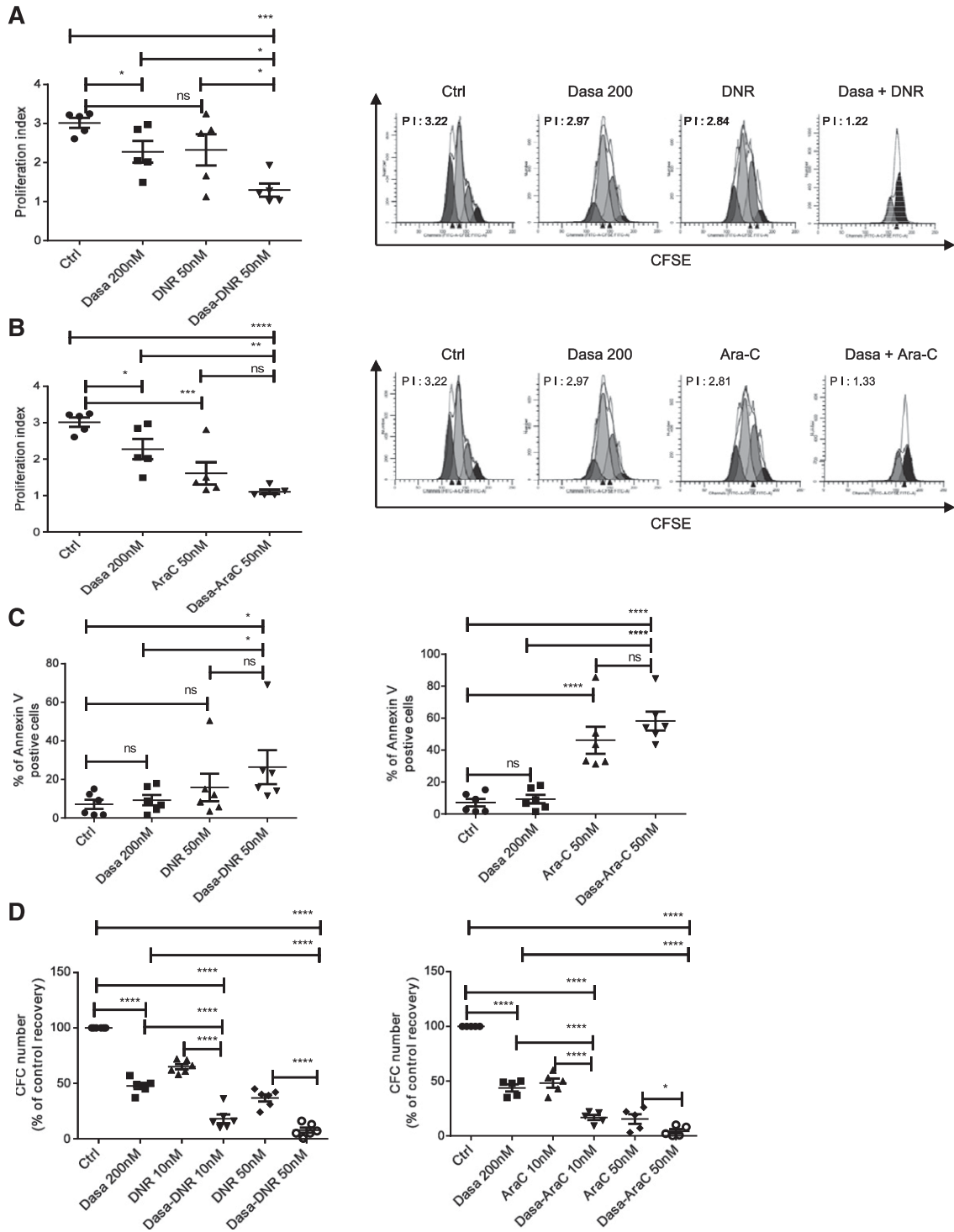


Figure 4. Dasatinib enhances apoptosis and inhibits cell proliferation in combination with chemotherapeutic agents in AML primitive and committed progenitors. AML CD34⁺ cells were labeled with CFSE, cultured for 72 hours either with dasatinib alone (200 nM), DNR alone (50 nM), or dasatinib (dasatinib 200 nM) in combination with DNR (A) or with Ara-C alone (50 nM) or dasatinib in combination with Ara-C (B). PI was determined using ModFit software, and proliferation indices were normalized to untreated controls. Histograms showing mean \pm SEM for proliferation of 5 AML is shown (left), and a representative CFSE cytometry flow plot indicating the calculated PI index is also shown (right). One-way ANOVA with posttest: ns, nonsignificant; * $P < .0465$; ** $P < .001$; *** $P < .003$; **** $P < .0001$. (C) Apoptosis of AML samples ($n = 6$) cultured for 72 hours with dasatinib alone (200 nM), DNR alone (50 nM), Ara-C alone (50 nM), or dasatinib (dasatinib 200 nM) in combination with DNR (left) and Ara-C (right). Results shown are presented as mean \pm SEM of Annexin V-positive cells for 6 AML samples. One-way ANOVA with posttest: ns, nonsignificant; * $P < .05$; **** $P < .0001$. (D) CFC generated from AML cells exposed for 48 hours to dasatinib alone (200 nM), DNR alone (10 and 50 nM; left, $n = 6$), Ara-C alone (10 and 50 nM; right, $n = 5$), or dasatinib in combination with DNR (left, $n = 6$) and Ara-C (right, $n = 5$). One-way ANOVA with posttest: * $P < .05$; **** $P < .0001$. Results shown are presented as percentage of control (mean \pm SEM).

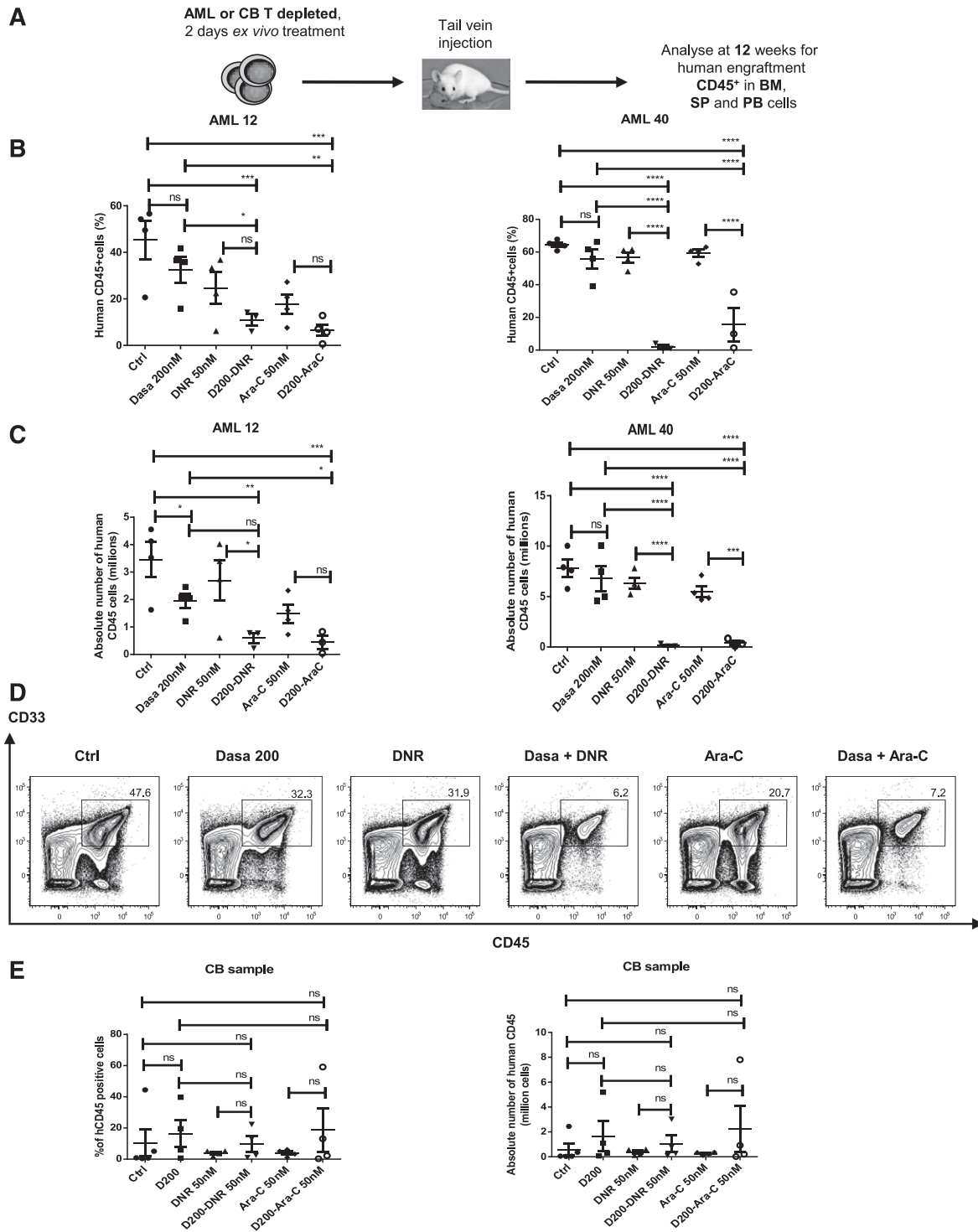


Figure 5. Combination of dasatinib with chemotherapeutic agents enhances elimination of human AML stem cells with NSG mouse repopulating capacity. (A) AML or CB primary MNCs were T-cell-depleted and cultured for 48 hours with dasatinib alone (200 nM), DNR alone (50 nM), Ara-C alone (50 nM), or D200 (dasatinib 200 nM) in combination with DNR and Ara-C and then transplanted via tail vein into sublethally irradiated 6- to 8-week-old NSG mice. After 12 weeks, BM, spleen (SP), and PB cells were analyzed by flow cytometry for expression of human CD45⁺. (B-C) Percentage (B) and absolute number (C) of human CD45⁺ engrafted cells in the BM at 12 weeks. Two different AML patients (AML 12 and AML 40) were used (n = 4 mice for untreated control, dasatinib, DNR, and Ara-C groups; n = 3 mice for the combination of dasatinib and Ara-C; n = 3 mice for the combination of dasatinib and DNR). One-way ANOVA with posttest: ns, nonsignificant; *P < .0392; **P < .0091; ****P < .0008; *****P < .0001. (D) Representative flow cytometry plot of CD45⁺ CD33⁺ cells engrafted in the BM. (E) Percentage (left) or absolute number (right) of human CB CD45⁺ engrafted cells in the BM at 12 weeks (n = 5 mice for untreated control; n = 4 for dasatinib, DNR, and Ara-C groups, combination of dasatinib and Ara-C; and n = 4 for the combination dasatinib and DNR). One-way ANOVA with posttest: ns, nonsignificant.

(50 nM), Ara-C (50 nM), or dasatinib plus DNR (50 nM) or Ara-C (50 nM) for 2 days were transplanted into NSG mice (Figure 5A). The combination of dasatinib with DNR or Ara-C significantly

reduced the percentage (Figure 5B) and absolute number (Figure 5C) of human CD45⁺ cells in murine BM at 12 weeks compared with dasatinib, DNR, or Ara-C alone and reduced CD34⁺ cells coexpressing

CD34, CD33, CD14, CD15, and CD11b (Figure 5D; supplemental Figure 4A-E). The combination of dasatinib with DNR or Ara-C did not inhibit engraftment of normal HSC compared with DNR or Ara-C alone (Figure 5E).

In vivo treatment with dasatinib and chemotherapeutic agents enhances LSC targeting

Because NSG mice tolerated chemotherapy poorly, we used an inversion 16 AML mouse model²² to evaluate in vivo effects of dasatinib and chemotherapy on AML LSC. The inversion 16 mutation results in expression of the CBF β -smooth muscle myosin heavy-chain²⁷ fusion protein that induces AML in cooperation with additional mutations.²² AML was induced by retroviral expression of *Mpl* in BM progenitors and transplantation into wild-type recipients.²³ Murine AML cells demonstrated increased *p*-SFK expression compared with control cells and were sensitive to inhibition by dasatinib treatment (supplemental Figure 5A). AML cells were transplanted into wild-type mice to induce leukemia. In the first experiment, mice were treated with dasatinib (10 mg/kg per day for 5 days), Ara-C (100 mg/kg per day for 5 days), and doxorubicin (3 mg/kg for 3 days)²⁸ or dasatinib combined with Ara-C and doxorubicin (Figure 6A). Doxorubicin was used because it is better tolerated than DNR, which causes severe toxicity when given intraperitoneally. Spleen size was reduced with dasatinib or doxorubicin plus Ara-C and was further reduced with the dasatinib and chemotherapy combination (Figure 6B). BM and spleen cellularity (supplemental Figure 5B) and leukemic GFP⁺ cells (Figure 6C) were reduced in mice treated with chemotherapy and further reduced with combination treatment. In a second experiment, mice were treated with dasatinib alone (10 mg/kg per day for 4 days), Ara-C (100 mg/kg per day for 4 days), and doxorubicin (3 mg/kg for 3 days) or dasatinib combined with Ara-C and doxorubicin. Again, significant reduction in leukemic GFP⁺ cells in BM and spleen was seen with chemotherapy, and further reduction was seen with combination treatment (data not shown). BM cells from treated mice were transplanted to secondary recipients. All mice receiving cells from control and dasatinib-treated mice died within 45 days (Figure 6D). In contrast, 45% (5/11) recipients of cells from mice treated with chemotherapy alone survived up to 240 days (end point). Recipients of cells from mice treated with the dasatinib and chemotherapy combination demonstrated significantly prolonged survival indicating improved targeting of AML LSC.

Treatment with dasatinib and chemotherapy enhances p53 signaling in AML CD34⁺ cells

DNR enhanced expression of p53 target genes in AML CD34⁺ cells only at high doses, whereas Ara-C did not activate p53 even at high doses (not shown). In contrast, addition of dasatinib to lower doses of DNR enhanced expression of p53 target genes, including BAX ($P = .01$), PUMA ($P = .03$), p21 ($P = .04$), NOXA ($P = .03$), and DR5 ($P = .01$) (Figure 7A) compared with DNR alone. Similar results were seen for dasatinib combined with Ara-C, although it was less marked than that seen for DNR (supplemental Figure 6A). Treatment with dasatinib and DNR also increased levels of p53 and the p53 target gene Bax on Western blotting and decreased myeloid cell leukemia sequence 1 (BCL2-related) (Figure 7B). Inhibition of p53 mRNA in AML CD34⁺ cells using siRNA (supplemental Figure 6B) significantly decreased apoptosis of cells treated with dasatinib plus chemotherapy, supporting a role for p53 in elimination of AML stem/progenitor cells by the combination (Figure 7C). A second siRNA targeting a different p53 sequence showed similar effects (supplemental Figure 6C). Combined LYN, HCK, and FGR knockdown as

well as c-KIT knockdown also resulted in significant increase in expression of p53 (Figure 7D) and the p53 target gene BAX (supplemental Figure 6D) in DNR-treated cells, showing that dasatinib's effects are mediated by SFK and c-KIT inhibition.

We did not see consistent changes in p53 serine 15 phosphorylation or lysine 382 acetylation after treatment with DNR, dasatinib, or the combination (not shown).^{29,30} In contrast, the combination resulted in reduced human mouse double minute 2 homolog (HDM2) serine 166 phosphorylation compared with DNR or dasatinib alone (Figure 7E; supplemental Figure 7A). Because HDM2 serine 166 phosphorylation is associated with enhanced p53 degradation, reduced phosphorylation could contribute to increased p53 in treated cells.³¹ The combination of dasatinib and DNR also enhanced inhibition of SFK phosphorylation in AML CD34⁺ CD38^{dim/-} and CD38⁺ cells (supplemental Figure 7B) and reduced AKT Thr 308 (Figure 7E; supplemental Figure 7A) and p42/44 mitogen-activated protein kinase (MAPK) phosphorylation (supplemental Figure 7C) in AML CD34⁺ cells compared with dasatinib or DNR alone, without impairing signal transducer and transcriptional activator 5 phosphorylation. Because AKT signaling enhances HDM2 Ser166 phosphorylation, reduced AKT activity in DNR plus dasatinib-treated cells may explain the observed reduction in HDM2 Ser166 phosphorylation. Indeed, AKT inhibition using LY2904002 also inhibited HDM2 Ser 166 phosphorylation in AML cells (supplemental Figure 7D) and reduced MAPK phosphorylation, whereas MAPK inhibition with PD98059 did not significantly affect AKT or HDM2 phosphorylation (not shown). In addition to effects on Akt, LY2904002 could also activate p53 by inhibiting ATM and ATR. Immunoprecipitation studies showed that dasatinib reduced p53 association with HDM2 in Molm13 AML cells (supplemental Figure 6E). Inhibition of p53-HDM2 interactions using Nutlin 3 also reduced AML progenitor growth and survival. Interestingly, dasatinib did not further enhance the effects of Nutlin 3 (supplemental Figure 6F-G), suggesting p53 activation was not increased in the presence of a strong HDM2 inhibitor. Overall, these experiments support a role for the modulation of HDM2-p53 interactions in enhanced targeting of chemotherapy-treated AML progenitors by dasatinib.

Discussion

Additional strategies to target AML LSC are required to improve patient outcomes. This study shows that the SFKs, LYN, HCK, and FGR are coexpressed and activated in AML stem/progenitor cells. SFKs and c-KIT contribute to AML stem/progenitor cell survival and proliferation, and inhibition of SFKs and c-KIT with dasatinib moderately reduces AML stem/progenitor cell growth and survival; importantly, dasatinib markedly enhances the sensitivity of AML stem/progenitor cells to chemotherapy. Our studies suggest that dasatinib enhances p53 activation in chemotherapy-treated AML cells via reduced AKT-mediated HDM2 phosphorylation. Dasatinib-mediated enhancement of LSC targeting by chemotherapeutic agents may represent an innovative therapeutic approach in AML.

We observed consistent expression of LYN and HCK and variable expression of FGR in AML CD34⁺ cells, indicating that individual samples coexpress more than a single SFK. Lack of correlation between SFK activity and cytogenetic risk group suggests SFK activation is associated with diverse molecular abnormalities. Activating SFK mutations are not reported in AML,^{32,33} and genetic loci for LYN, HCK or FGR are not hot spots for translocations, although a novel TEL-LYN fusion gene was reported in primary myelofibrosis.³⁴ SFKs may be activated downstream of FLT3,¹⁵ c-KIT mutations,³⁵

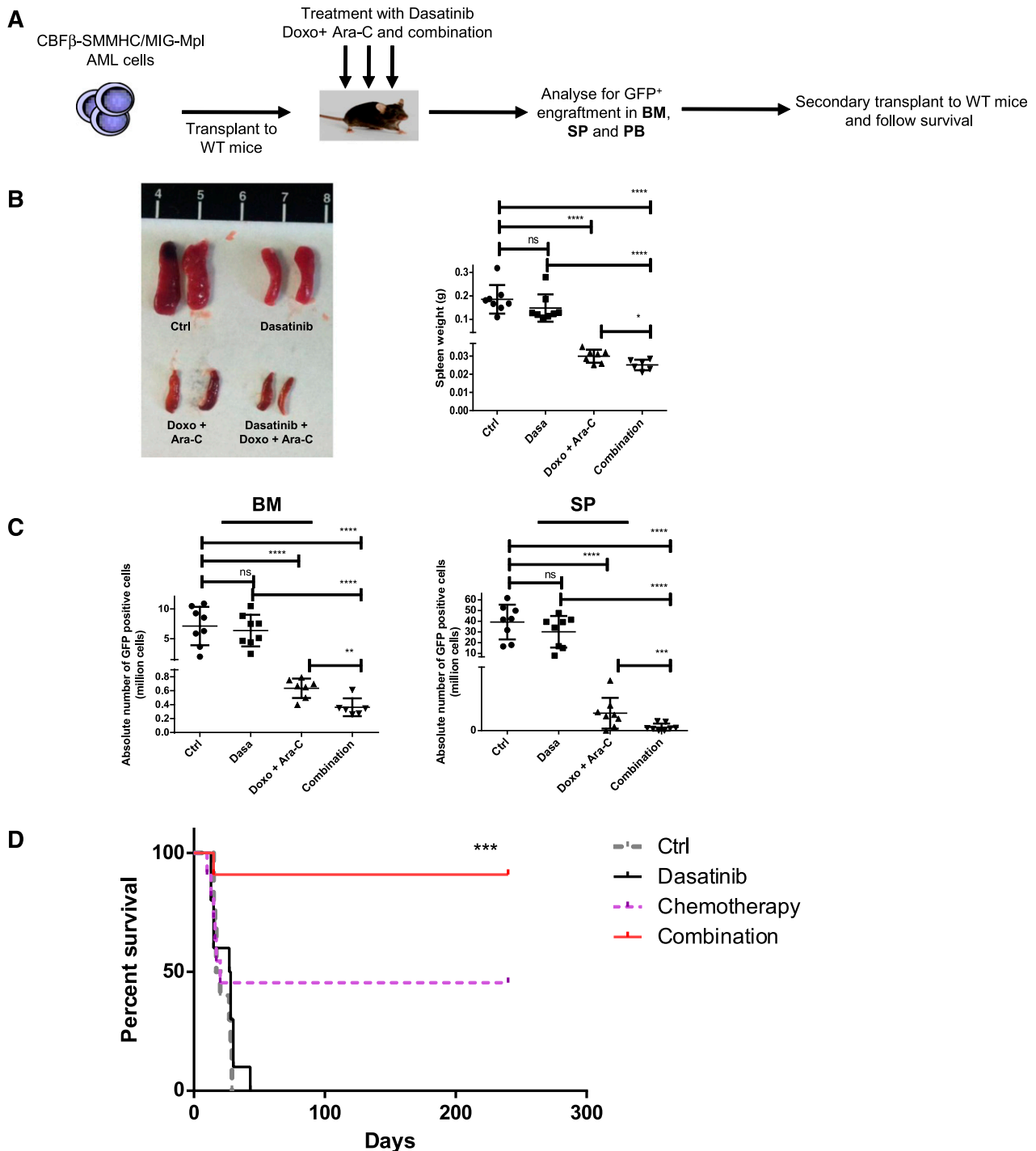


Figure 6. In vivo administration of dasatinib combined with chemotherapeutic agents enhances elimination of AML stem cells in a murine AML model. (A) Murine AML cells (5×10^4) coexpressing CBF β -smooth muscle myosin heavy-chain and murine stem cell virus-internal ribosome entry site-green fluorescent protein-myeloproliferative leukemia virus oncogene (MIG-Mpl) were injected to wild-type C57BL/6N mice via tail vein. Mice were treated 7 to 10 days posttransplantation with dasatinib alone (10 mg/kg per day) for 5 days, Ara-C (100 mg/kg per day) for 5 days with doxorubicin (3 mg/kg) for 3 days, or the combination of dasatinib with Ara-C and doxorubicin for 5 days. Untreated mice were studied as controls. AML engraftment was assessed by the percentage of GFP $^{+}$ cells in the BM, SP, and PB. BM cells were injected for secondary transplant and mice were followed-up for survival for 240 days. (B) Representative images for the spleen from mice treated in vivo (left) and histogram showing the spleen weight (right). In the different groups (control and dasatinib, $n = 8$; doxo + Ara-C group, $n = 7$; and combination group, $n = 6$). One-way ANOVA with posttest: ns, nonsignificant; * $P < .05$; **** $P < .0001$. (C) Absolute number of GFP $^{+}$ cells in BM (left) and SP (right) in each treatment groups. One-way ANOVA with posttest: ns, nonsignificant; ** $P < .039$; *** $P < .001$; **** $P < .0001$. (D) Survival curve of mice receiving secondary transplantation of equal numbers of BM cells from control or treated mice (control 900 GFP $^{+}$ cells/mouse, dasatinib 8550 GFP $^{+}$ cells/mouse, chemotherapy 1195 GFP $^{+}$ cells/mouse, dasatinib plus chemotherapy 1160 GFP $^{+}$ cells/mouse). Mice were followed-up for survival up to 240 days (control and dasatinib group, $n = 10$; doxo + Ara-C and combination group, $n = 11$); *** $P < .001$ (Mantel-Cox test).

or RTK fusion proteins or in response to GF signaling in AML cells. However, we did not find a significant association between SFK activation and the FLT3-ITD mutation. SFK activity is regulated by

phosphorylation,^{10,36} and negative regulators including CBL,^{37,38} SOCS, or SHP-1^{39,40} may be reduced in AML cells. We observed low levels of phosphorylation at the negative regulatory Y527 site

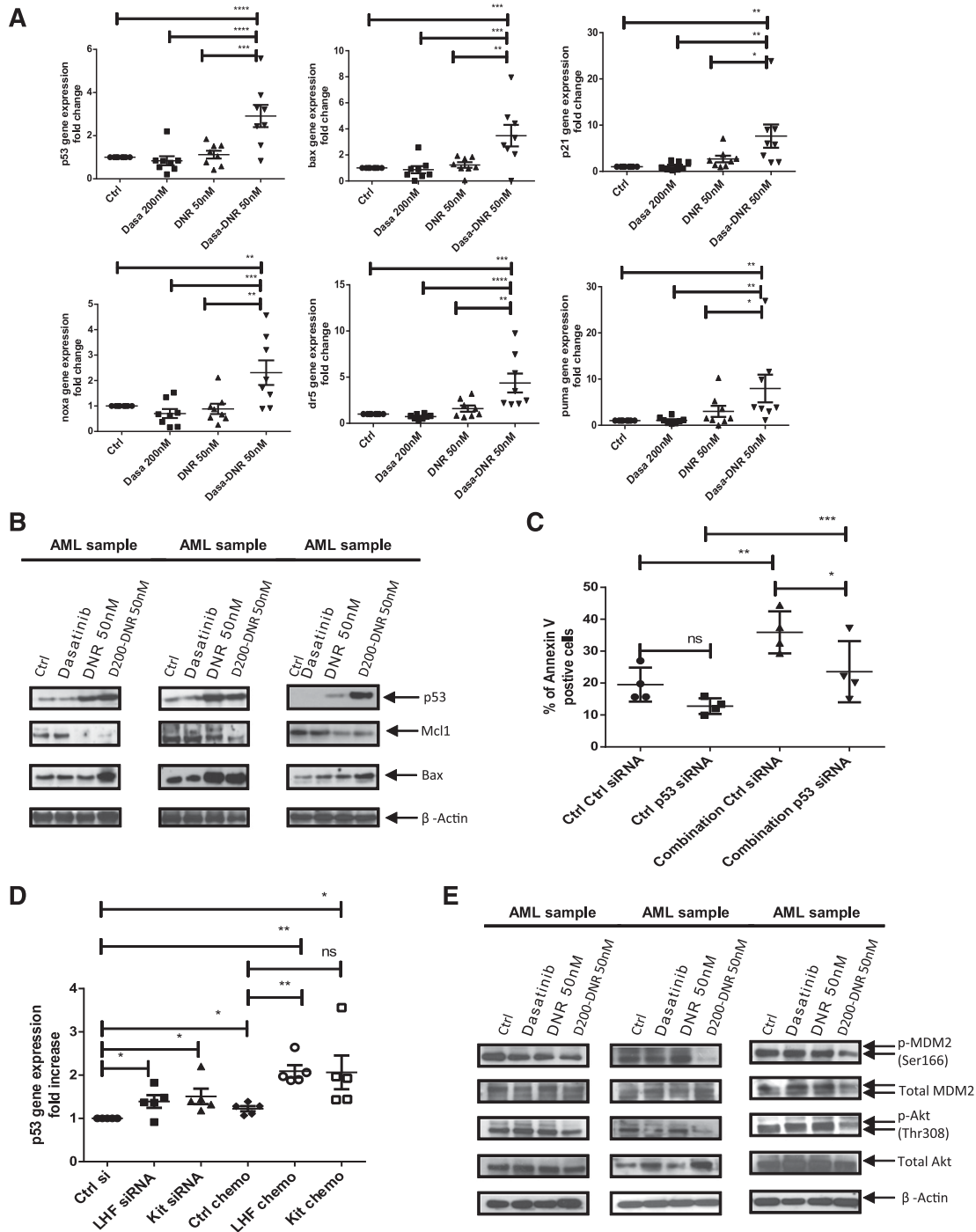


Figure 7. Dasatinib combined with chemotherapy enhances p53 transcriptional activity and modulates the Akt-HDM2 axis in AML CD34⁺ cells. (A) Quantitative PCR analysis of p53 and p53 target genes in primary AML CD34⁺ cells exposed for 16 hours to dasatinib alone (200 nM), DNR alone (50 nM), or dasatinib 200 nM in combination with DNR. β -2M was used as an internal control and results shown are expressed as mean \pm SEM of 8 AML samples. One-way ANOVA with posttest: ns, nonsignificant; * P < .05; ** P < .01; *** P < .001; **** P < .0001. (B) Western blot analysis for AML samples exposed for 48 hours to dasatinib alone (200 nM), DNR alone (50 nM), or dasatinib in combination with DNR. Indicated antibodies are listed and β -actin was used as a loading control. Results shown are representative of 7 AML samples analyzed. (C) Twenty-four hours postnucleofection, AML samples ($n = 4$) were treated without or with dasatinib (200 nM) + DNR (50 nM) and assayed for apoptosis after 2 more days. Results shown are presented as mean percentages \pm SEM of Annexin V-positive cells in control versus p53 siRNA and in treated versus untreated cells. * P < .0201; ** P < .0039; *** P < .0003. (D) Twenty-four hours postnucleofection with indicated siRNA, AML samples ($n = 5$) were treated without or with dasatinib (200 nM) + DNR (50 nM) for 16 hours and p53 gene expression was assessed using quantitative PCR analysis. β 2M was used as an internal control; results shown are expressed as mean \pm SEM of 5 AML samples. ns, nonsignificant; * P < .0278; ** P < .0072. (E) Western blot analysis for AML samples exposed for 2 hours to dasatinib alone (200 nM), DNR alone (50 nM) or dasatinib in combination with DNR. Indicated antibodies are listed and β -actin was used as a loading control. Results shown are representative of 7 AML samples analyzed.

relative to the Y416 activation site. Finally, high SFK levels could reflect reduced degradation through calpain or the ubiquitin-proteasome system.⁴¹

Knockdown of LYN and HCK, and to a lesser extent FGR, enhanced AML progenitor apoptosis and impaired CFC growth, consistent with the coexpression of these kinases in AML CD34+

cells and with observations that SFKs contribute to AML cell survival and growth.^{13,14} Because SFKs are highly homologous, they may compensate for each other, and combined inhibition of the 3 SFKs resulted in greater inhibition of AML progenitors. The SFK inhibitor dasatinib, with activity against LYN, HCK, and FGR, was effective in inhibiting AML stem/progenitor cell growth and survival. SFKs may contribute to LSC viability through several signaling mechanisms, including the MAPK and PI3K/Akt pathways. Inhibition of c-KIT also reduces AML LSC growth and survival and likely contributes to dasatinib effects. Therefore, targeting of multiple kinases may be an added benefit of dasatinib treatment.⁴² The complex molecular alterations in primary human LSC, interpatient variability, and complicated effects of multikinase inhibition on interconnected signaling networks make it difficult to specify the precise mechanisms underlying dasatinib effects.

Dasatinib monotherapy has not been successful in clinical trials in solid tumors and hematologic malignancies⁴³ other than chronic myeloid leukemia. Dasatinib as a single agent had only moderate inhibitory effects on AML LSC. However, dasatinib markedly enhanced targeting of AML LSC by DNR and Ara-C both in vitro and in vivo. Sensitization to chemotherapeutic agents was associated with enhanced expression of p53 and p53 target genes. The inhibitory effects of dasatinib plus chemotherapy on AML cells were reversed by p53 knockdown. Our results suggest that although the p53 axis is intact, p53 activation in response to chemotherapy is impaired in AML CD34⁺ cells, and dasatinib can enhance p53-mediated elimination of AML LSC by chemotherapy. Activation of p53 via HDM2 inhibition also inhibited AML progenitors.⁴⁴ Although cell cycle inhibition by dasatinib could theoretically reduce sensitivity to apoptosis, p53 activation may induce apoptosis even in quiescent progenitors.

Mutations in p53 are rare in AML, except with complex karyotypes.⁴⁵ The PI3K/AKT signaling pathway is activated in from 50% to 91% of primary AML samples, and AKT-mediated phosphorylation of HDM2 may suppress p53 activation.^{46,47} Combined dasatinib and DNR treatment reduced AKT-mediated HDM2 phosphorylation. The dasatinib and DNR combination also inhibited MAPK phosphorylation in AML progenitors. Because MAPK signaling can also attenuate the p53 response, MAPK inhibition may represent an additional mechanism contributing to p53 activation. Given the observation that dasatinib did not effectively inhibit AKT signaling in AML progenitors by itself but effectively inhibited AKT signaling in combination with DNR, it appears that DNR modulates pathways allowing persistent AKT signaling in dasatinib-treated cells. DNR can alter cell signaling through sphingomyelin-ceramide, MAPK, c-Jun N-terminal kinase, nuclear factor κ B, and PI3K/AKT pathways⁴⁸ and can inactivate AKT signaling in muscle cells.⁴⁹ The specific mechanisms underlying

cooperativity between dasatinib and DNR in AML cells require additional investigation, although DNR treatment did modestly increase SFK inhibition in combination with dasatinib. Mechanisms other than p53 activation may also contribute to cooperativity. For example, the combination of dasatinib and DNR enhanced inhibition of topoisomerase II α (not shown), which could be an additional mechanism of synergy.

Our results support clinical trials to explore whether addition of dasatinib to chemotherapeutic regimens can enhance targeting of AML LSC. Ongoing clinical trials adding dasatinib with chemotherapy are directed toward AML with core-binding factor mutations, with the rationale of targeting associated c-Kit mutations. On the basis of our results, we are initiating a clinical trial combining dasatinib with chemotherapy to improve outcomes in poor-risk AML patients, with the novel rationale of enhancing AML LSC sensitivity to chemotherapy. Our studies also support evaluation of combinations of dasatinib with other agents whose activity may be limited by impaired p53 signaling, as well as other approaches to enhance p53 activity in AML LSC.

Acknowledgments

The authors thank Jennifer Arceo and Linda Seymour for assistance with obtaining samples.

This work was supported by a grant from the Hoag foundation. The authors thank StemCyte for their gift of CB samples. The authors acknowledge the support of the Animal Resources Center.

Authorship

Contribution: C.D.S. designed and performed research, collected and analyzed data, and wrote the paper; T.M., Y.W.H., H.L., and A.L. performed research and reviewed the paper; S.J.F. contributed materials and reviewed the paper; Y.-H.K. designed research, analyzed and interpreted data, and wrote the paper; and R.B. designed research, analyzed and interpreted data, and wrote the paper.

Conflict-of-interest disclosure: R.B. is on the advisory board and receives honoraria from Bristol-Myers Squibb. The remaining authors declare no competing financial interests.

Correspondence: Ravi Bhatia, Division of Hematopoietic Stem Cell and Leukemia Research, Department of Hematology and HCT, City of Hope National Medical Center, Duarte, CA 91010; e-mail: rbhatia@coh.org.

References

- Tallman MS, Gilliland DG, Rowe JM. Drug therapy for acute myeloid leukemia. *Blood*. 2005;106(4):1154-1163.
- Bonnet D, Dick JE. Human acute myeloid leukemia is organized as a hierarchy that originates from a primitive hematopoietic cell. *Nat Med*. 1997;3(7):730-737.
- Reya T, Morrison SJ, Clarke MF, Weissman IL. Stem cells, cancer, and cancer stem cells. *Nature*. 2001;414(6859):105-111.
- Sarry JE, Murphy K, Perry R, et al. Human acute myelogenous leukemia stem cells are rare and heterogeneous when assayed in NOD/SCID/IL2R γ c-deficient mice. *J Clin Invest*. 2011;121(1):384-395.
- Eppert K, Takenaka K, Lechman ER, et al. Stem cell gene expression programs influence clinical outcome in human leukemia. *Nat Med*. 2011;17(9):1086-1093.
- Huntly BJ, Gilliland DG. Leukaemia stem cells and the evolution of cancer-stem-cell research. *Nat Rev Cancer*. 2005;5(4):311-321.
- Récher C, Dos Santos C, Demur C, Payrastré B. mTOR, a new therapeutic target in acute myeloid leukemia. *Cell Cycle*. 2005;4(11):1540-1549.
- Zheng R, Klang K, Gorin NC, Small D. Lack of KIT or FMS internal tandem duplications but co-expression with ligands in AML. *Leuk Res*. 2004;28(2):121-126.
- Thomas SM, Brugge JS. Cellular functions regulated by Src family kinases. *Annu Rev Cell Dev Biol*. 1997;13:513-609.
- Kim LC, Song L, Haura EB. Src kinases as therapeutic targets for cancer. *Nat Rev Clin Oncol*. 2009;6(10):587-595.
- Ptasznik A, Nakata Y, Kalota A, Emerson SG, Gewirtz AM. Short interfering RNA (siRNA) targeting the Lyn kinase induces apoptosis in primary, and drug-resistant, BCR-ABL1(+) leukemia cells. *Nat Med*. 2004;10(11):1187-1189.

12. Contri A, Brunati AM, Trentin L, et al. Chronic lymphocytic leukemia B cells contain anomalous Lyn tyrosine kinase, a putative contribution to defective apoptosis. *J Clin Invest*. 2005;115(2):369-378.
13. Dos Santos C, Demur C, Bardet V, Prade-Houdellier N, Payrastra B, Récher C. A critical role for Lyn in acute myeloid leukemia. *Blood*. 2008;111(4):2269-2279.
14. Saito Y, Kitamura H, Hijikata A, et al. Identification of the therapeutic targets for quiescent, chemotherapy-resistant human leukemia stem cells. *Sci Transl Med*. 2010;2(17):ra9.
15. Okamoto M, Hayakawa F, Miyata Y, et al. Lyn is an important component of the signal transduction pathway specific to FLT3/ITD and can be a therapeutic target in the treatment of AML with FLT3/ITD. *Leukemia*. 2007;21(3):403-410.
16. Ozawa Y, Williams AH, Estes ML, et al. Src family kinases promote AML cell survival through activation of signal transducers and activators of transcription (STAT). *Leuk Res*. 2008;32(6):893-903.
17. Amrein PC. The potential for dasatinib in treating chronic lymphocytic leukemia, acute myeloid leukemia, and myeloproliferative neoplasms. *Leuk Lymphoma*. 2011;52(5):754-763.
18. Bhatia R, McGlave PB, Miller JS, Wissink S, Lin WN, Verfaillie CM. A clinically suitable ex vivo expansion culture system for LTC-IC and CFC using stroma-conditioned medium. *Exp Hematol*. 1997;25(9):980-991.
19. Jordan CT, Yamasaki G, Minamoto D. High-resolution cell cycle analysis of defined phenotypic subsets within primitive human hematopoietic cell populations. *Exp Hematol*. 1996;24(11):1347-1355.
20. Zhang B, Strauss AC, Chu S, et al. Effective targeting of quiescent chronic myelogenous leukemia stem cells by histone deacetylase inhibitors in combination with imatinib mesylate. *Cancer Cell*. 2010;17(5):427-442.
21. Ishikawa F, Yoshida S, Saito Y, et al. Chemotherapy-resistant human AML stem cells home to and engraft within the bone-marrow endosteal region. *Nat Biotechnol*. 2007;25(11):1315-1321.
22. Kuo YH, Landrette SF, Heilman SA, et al. Cbf beta-SMMHC induces distinct abnormal myeloid progenitors able to develop acute myeloid leukemia. *Cancer Cell*. 2006;9(1):57-68.
23. Landrette SF, Madera D, He F, Castilla LH. The transcription factor Plagl2 activates Mpl transcription and signaling in hematopoietic progenitor and leukemia cells. *Leukemia*. 2011;25(4):655-662.
24. O'Donnell MR, Abboud CN, Altman J, et al; National Comprehensive Cancer Network. Acute myeloid leukemia. *J Natl Compr Canc Netw*. 2011;9(3):280-317.
25. Schittenhelm MM, Shiraga S, Schroeder A, et al. Dasatinib (BMS-354825), a dual SRC/ABL kinase inhibitor, inhibits the kinase activity of wild-type, juxtamembrane, and activation loop mutant KIT isoforms associated with human malignancies. *Cancer Res*. 2006;66(1):473-481.
26. Christopher LJ, Cui D, Wu C, et al. Metabolism and disposition of dasatinib after oral administration to humans. *Drug Metab Dispos*. 2008;36(7):1357-1364.
27. Liu P, Tarié SA, Hajra A, et al. Fusion between transcription factor CBF beta/PEBP2 beta and a myosin heavy chain in acute myeloid leukemia. *Science*. 1993;261(5124):1041-1044.
28. Zuber J, Radtke I, Pardee TS, et al. Mouse models of human AML accurately predict chemotherapy response. *Genes Dev*. 2009;23(7):877-889.
29. Dumaz N, Meek DW. Serine15 phosphorylation stimulates p53 transactivation but does not directly influence interaction with HDM2. *EMBO J*. 1999;18(24):7002-7010.
30. Prives C, Manley JL. Why is p53 acetylated? *Cell*. 2001;107(7):815-818.
31. Zhou BP, Liao Y, Xia W, Zou Y, Spohn B, Hung MC. HER-2/neu induces p53 ubiquitination via Akt-mediated MDM2 phosphorylation. *Nat Cell Biol*. 2001;3(11):973-982.
32. Loriaux MM, Levine RL, Tyner JW, et al. High-throughput sequence analysis of the tyrosine kinase in acute myeloid leukemia. *Blood*. 2008;111(9):4788-4796.
33. Tomasson MH, Xiang Z, Walgren R, et al. Somatic mutations and germline sequence variants in the expressed tyrosine kinase genes of patients with de novo acute myeloid leukemia. *Blood*. 2008;111(9):4797-4808.
34. Tanaka H, Takeuchi M, Takeda Y, et al. Identification of a novel TEL-Lyn fusion gene in primary myelofibrosis. *Leukemia*. 2010;24(1):197-200.
35. Shivakrupa R, Linnekin D. Lyn contributes to regulation of multiple Kit-dependent signaling pathways in murine bone marrow mast cells. *Cell Signal*. 2005;17(1):103-109.
36. Brdicka T, Pavlistová D, Leo A, et al. Phosphoprotein associated with glycosphingolipid-enriched microdomains (PAG), a novel ubiquitously expressed transmembrane adaptor protein, binds the protein tyrosine kinase csk and is involved in regulation of T cell activation. *J Exp Med*. 2000;191(9):1591-1604.
37. Caligiuri MA, Briesewitz R, Yu J, et al. Novel c-CBL and CBL-b ubiquitin ligase mutations in human acute myeloid leukemia. *Blood*. 2007;110(3):1022-1024.
38. Sargin B, Choudhary C, Crosetto N, et al. FLT3-dependent transformation by inactivating c-Cbl mutations in AML. *Blood*. 2007;110(3):1004-1012.
39. Watanabe D, Ezoe S, Fujimoto M, et al. Suppressor of cytokine signalling-1 gene silencing in acute myeloid leukaemia and human haematopoietic cell lines. *Br J Haematol*. 2004;126(5):726-735.
40. Johan MF, Bowen DT, Frew ME, Goodeve AC, Reilly JT. Aberrant methylation of the negative regulators RASSF1A, SHP-1 and SOCS-1 in myelodysplastic syndromes and acute myeloid leukaemia. *Br J Haematol*. 2005;129(1):60-65.
41. Ma W, Kantarjian H, Zhang X, et al. Ubiquitin-proteasome system profiling in acute leukemias and its clinical relevance. *Leuk Res*. 2011;35(4):526-533.
42. Guerrouahen BS, Futami M, Vavilavala C, et al. Dasatinib inhibits the growth of molecularly heterogeneous myeloid leukemias. *Clin Cancer Res*. 2010;16(4):1149-1158.
43. Montero JC, Seoane S, Ocaña A, Pandiella A. Inhibition of SRC family kinases and receptor tyrosine kinases by dasatinib: possible combinations in solid tumors. *Clin Cancer Res*. 2011;17(17):5546-5552.
44. Kojima K, Konopleva M, Samudio IJ, et al. MDM2 antagonists induce p53-dependent apoptosis in AML: implications for leukemia therapy. *Blood*. 2005;106(9):3150-3159.
45. Rücker FG, Schlenk RF, Bullinger L, et al. TP53 alterations in acute myeloid leukemia with complex karyotype correlate with specific copy number alterations, monosomal karyotype, and dismal outcome. *Blood*. 2012;119(9):2114-2121.
46. Xu Q, Simpson SE, Scialla TJ, Bagg A, Carroll M. Survival of acute myeloid leukemia cells requires PI3 kinase activation. *Blood*. 2003;102(3):972-980.
47. Sujobert P, Bardet V, Cornillet-Lefebvre P, et al. Essential role for the p110delta isoform in phosphoinositide 3-kinase activation and cell proliferation in acute myeloid leukemia. *Blood*. 2005;106(3):1063-1066.
48. Laurent G, Jaffrézou JP. Signaling pathways activated by daunorubicin. *Blood*. 2001;98(4):913-924.
49. Stulpinas A, Imbrasaitė A, Kalvelytė AV. Daunorubicin induces cell death via activation of apoptotic signalling pathway and inactivation of survival pathway in muscle-derived stem cells. *Cell Biol Toxicol*. 2012;28(2):103-114.